Bioorganic & Medicinal Chemistry Letters 24 (2014) 2546–2554

Contents lists available at ScienceDirect

Bioorganic & Medicinal Chemistry Letters

journal homepage: www.elsevier.com/locate/bmcl

BMCL Digest

Hot spot-based design of small-molecule inhibitors for protein–protein interactions

Wenxing Guo, John A. Wisniewski, Haitao Ji *

Department of Chemistry, Center for Cell and Genome Science, University of Utah, 315 South 1400 East, Salt Lake City, UT 84112-0850, USA

ARTICLE INFO

Article history:
Received 6 January 2014
Revised 26 March 2014
Accepted 28 March 2014
Available online 5 April 2014

Keywords:
Protein–protein interactions
Inhibitor
Hot spots
Rational design
Selectivity

ABSTRACT

Protein–protein interactions (PPIs) are important targets for the development of chemical probes and therapeutic agents. From the initial discovery of the existence of hot spots at PPI interfaces, it has been proposed that hot spots might provide the key for developing small-molecule PPI inhibitors. However, there has been no review on the ways in which the knowledge of hot spots can be used to achieve inhibitor design, nor critical examination of successful examples. This Digest discusses the characteristics of hot spots and the identification of druggable hot spot pockets. An analysis of four examples of hot spot-based design reveals the importance of this strategy in discovering potent and selective PPI inhibitors. A general procedure for hot spot-based design of PPI inhibitors is outlined.

Protein–protein interactions (PPIs) play a pivotal role in most biological processes. The interface between two proteins typically has an area of 1500–3000 Å^2 with approximately 750–1500 Å^2 of surface area buried in each protein.[1–3] The formation of a protein–protein complex is largely driven by hydrophobic effects,[4] which occur between the nonpolar regions of protein residues through van der Waals contacts. Electrostatic complementarity of the interacting protein surfaces between two proteins promotes the formation and lifetime of the complex. For some interfaces hydrogen bonding and electrostatic interaction play a major role in steering one protein to dock onto the binding site of the second protein.

Characteristics of hot spots and hot regions: The residues on the protein–protein interface do not contribute equally to PPIs. A small subset of residues contribute to the majority of the binding free energy; they are called hot spots.[5] A hot spot is defined as a residue which substitution by an alanine leads to a significant decrease in the free energy of binding ($\Delta\Delta G_{binding} > 1.5$ kcal/mol).[5] The experiment that involves individually mutating interface residues to alanine, eliminating side-chain atoms beyond C_β, and then measuring the effect of individual side chain on binding affinity is called alanine scanning. A survey of alanine scanning data indicated that the amino acid composition of hot spots was enriched in tryptophan (W), arginine (R), and tyrosine (Y).[6] This trend of residue enrichment was also reproduced by a different surface analysis approach using clustered interface families.[7] Energetic hot spots from alanine scanning correlate with structurally conserved residues.[8] The number of the structurally conserved residues, in particular the energetic hot spots, increases with the expansion of the interacting surface area. Typically, hot spot density on the protein–protein interface composes 10% of the binding site residues.[9]

The free energy of binding between two proteins is not a simple summation of the contribution from individual hot spots. Hot spots tend to occur in clusters. Within the cluster, the tightly packed hot spots are in contact with each other and form a network of conserved interactions called hot regions.[10] One example of hot regions in a protein–protein interface is shown in Figure 1. The contributions of hot spots within one hot region are cooperative to stabilize PPIs. Hot regions are networked and contribute dominantly to the stability of PPIs. The energetic contributions between two hot regions can be additive[11] or cooperative.[12]

The protruding hot region of one protein packs against the concave hot region of the other protein.[4,13] Figure 2 illustrates a typical arrangement of hot spot and hot region. Residues 1–4 in Figure 2 constitute the top hot region for the interactions between proteins A and B while residues 5–8 form the bottom hot region. For the top hot region residues 1 and 3 make a protruding hot region, and residues 2 and 4 create a concave hot region. The projecting hot spot, residue 1 in Figure 2, makes a direct contact with hot spot 2 in the concave hot spot pocket. Residue 3 organizes the orientation of projecting hot spot 1, and 4 supports the structure of the hot spot pocket. Not only the alanine mutations of hot spots 1 and 2 but also

* Corresponding author. Tel.: +1 (801) 581 6747; fax: +1 (801) 581 8433.
E-mail address: markji@chem.utah.edu (H. Ji).

http://dx.doi.org/10.1016/j.bmcl.2014.03.095
0960-894X/

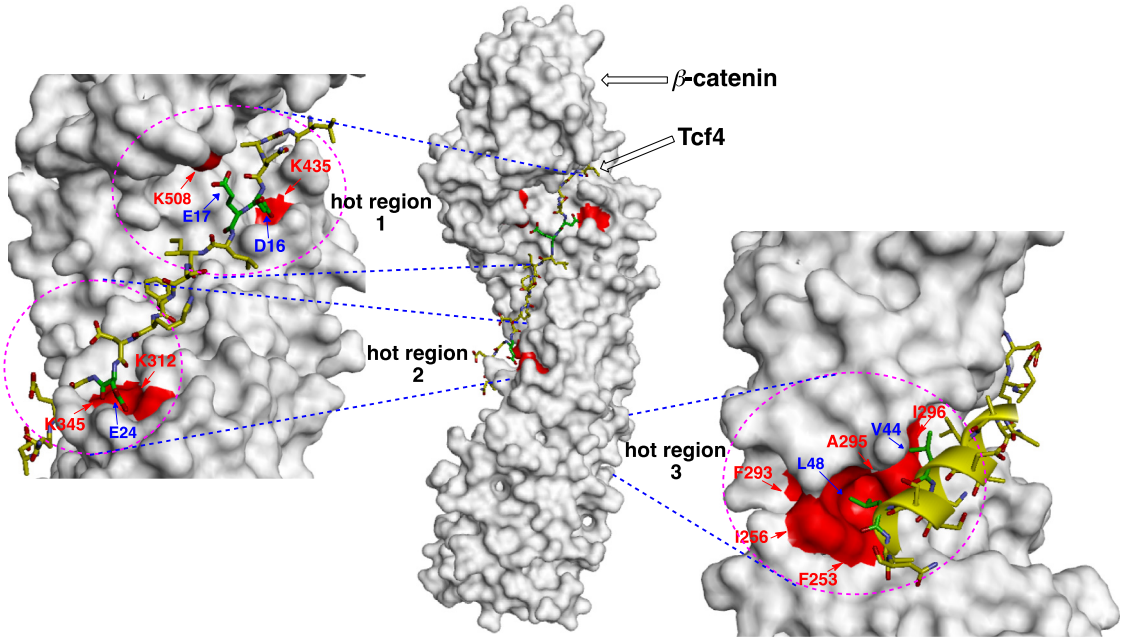

Figure 1. Crystal structure of β-catenin in complex with T-cell factor (Tcf) shows three hot regions (PDB IDs, 1G3J and 2GL7). Hot region 1 includes K435 and K508 of β-catenin and D16 and E17 of Tcf4. Hot region 2 includes K312 and K345 of β-catenin and E24 and E29 of Tcf4. Hot region 3 includes F253, I256, F293, A295, and I296 of β-catenin and V44 and L48 of Tcf4.

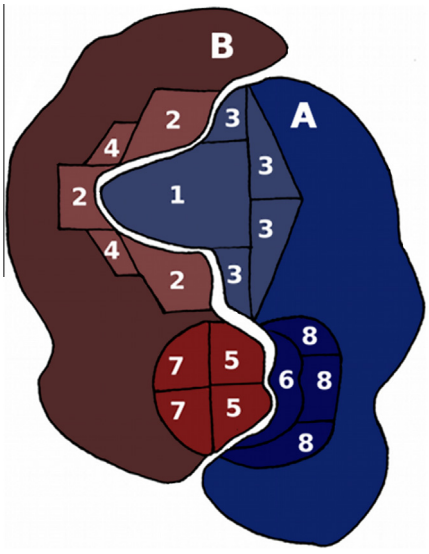

Figure 2. Illustration of hot spots and hot regions in the protein–protein interface (adapted from Golden et al.[13]). The top hot region has a projecting hot spot, **1**, from protein A. This projecting residue binds to a complementary surface pocket of protein B, which is lined by residues that are labeled **2**. The residues on protein A that help to orient projecting hot spot **1** are labeled **3**. The residues on protein B that help to form the concave hot region are labeled **4**. The bottom hot region has two projecting hot spots from protein B that are labeled **5**. The concave surface pocket residue of protein A is labeled **6**. The residues in protein B that support the projecting hot spot are labeled **7**. The residues in protein A that support the formation of the concave hot region are labeled **8**.

the mutations of residues 3 and 4 would greatly affect the free energy of binding between proteins A and B. Therefore, residues 1–4 are all called energetic hot spots in the alanine scanning experiments. The projecting hot spots, 1 and 5 in Figure 2, are also named anchor residues if the change of their solvent accessible surface areas (SASA) upon binding is >0.5 Å^2. [14,15]

The concave hot regions are usually pre-organized in the unbound state prior to protein complexation,[14,16] as demonstrated in Figure 3. The existence of such ready-made recognition motifs implies that the binding pathway can avoid kinetically costly structural rearrangement at the core of the binding interface, allowing for a relatively smooth recognition process. Once the protruding hot region is docked to the concave hot region, an induced fit process further contributes to the formation of the final high-affinity complex.

Alanine scanning experiments to unravel hot spots are relatively time-consuming and labor-intensive. In some cases, the results of the alanine scanning experiments could be inconclusive. For example, the alanine mutation of residues that participate in forming concave hot regions likely gives rise to nonadditive $\Delta\Delta G_{binding}$ values. The alanine mutations could affect the free energy of binding by a mechanism unrelated to the PPIs at the interface, for example, by destabilizing the unbound state of the protein or altering its conformation. Therefore, hot spots identified by alanine scanning experiments could be false positives in the sense that they do not reflect energetically important binding interactions with the partner protein. In addition, alanine scans could miss a binding hot spot that mostly involves interaction of backbone rather than side-chain atoms. Computational methods have been developed to predict hot spots. These methods are complementary to the alanine scanning experiments and provide valuable insights into the nature of protein–protein complexation.[17] Some computational methods calculate the changes of free energy of binding upon mutation using calibrated free energy functions, such as Robetta[18] and FOLDEF.[19] A second group of computational methods incorporate molecular dynamics simulations in computational alanine scanning.[20] The third group covers knowledge-based methods that learn the relationship between hot spots and various residue features from training data, and then predict new hot spots.[21] Also, hybrid approaches, which integrate the strengths of the machine learning and energy-based methods, have been developed and applied to predict protein hot spots.[22]

Solvation also plays an important role in protein–protein association. Hot spots are often surrounded by energetically less important residues that shape like an O-ring to occlude bulk water molecules from the hot spot.[6] The affinity of a hot region depends not only on the energetically critical hot spots located near the

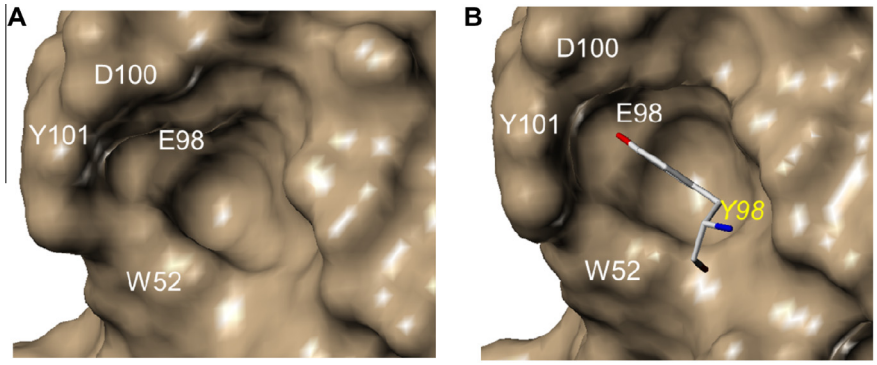

Figure 3. Pre-organization of the concave hot region in the protein–protein interface. The anti-hen-egg-white lysozyme antibody D1.3/anti-idiotopic antibody E5.2 complex was used as an example.[16] Examination of the two structures reveals that the concave region of D1.3 is formed in both the absence and presence of E5.2. (A) The crystal structure of the apo antibody D1.3 (PDB id, 1VFB). (B) The crystal structure of the complex of antibodies D1.3 and E5.2 (PDB id, 1DVF).

center of a hot region but also on the surrounding seal of contacting residues that establish the correct solvation environment. The O-ring structure results in a lower local dielectric constant environment and an enhancement of specific electrostatic and hydrogen bond interactions for the polar and ionizable hot spots. The further development of the O-ring structure led to the 'double water exclusion' hypothesis. This hypothesis not only recognizes the existence of the hydrophobic O-ring structure but also assumes some hot spots themselves are water-free.[23] Both the O-ring theory[24] and the 'double water exclusion' hypothesis[23,25] explain certain PPIs.

Druggable hot spot pockets: Protein–protein interfaces have been recognized as biologically appealing targets for designing small-molecule chemical probes and/or therapeutic agents. However, the discovery of such small molecules with desired potency, selectivity, and physicochemical properties has proven challenging.[2,3] Protein–protein interfaces tend to be flat, featureless, and rather large (typically 1500–3000 Å^2); while the surface of a protein often displays complex dynamic behavior. In contrast to enzymes or receptors that have one or two disproportionately large substrate-binding pockets with an average volume of 260 Å^3, protein–protein interfaces are characterized by several shallow small pockets with an average volume of 54 Å^3 for each pocket.[26] These features make the discovery of potent PPI inhibitors difficult. Nevertheless, the pre-existence of the concave hot spot region on the unbound protein surface and the complementary packing of two hot regions from two interacting proteins provide impetus to search for small-molecule PPI inhibitors. A small-molecule PPI inhibitor should target 3–5 small pockets in the protein–protein surface and take advantage of protein adaptability.[26] The conformational adaptivity of a protein surface has frequently been observed when binding with a second protein or a small molecule.[3] It is possible that the protein surface adjacent to a concave hot region undergoes induced-fit to accommodate small-molecule PPI inhibitors.

Hot spot pockets for PPIs are distinguishable from the other regions of protein surface due to their concave topology combined with a pattern of hydrophobic and polar functionality. This combination of properties confers on concave hot regions a tendency to bind small organic compounds possessing some polar functionality decorating a largely hydrophobic scaffold. In other words, concave hot regions on PPI surfaces are not simply the sites that are complementary to a particular organic functionality but rather possess a general tendency to bind organic compounds with a variety of structures. This property of hot regions has been observed in Multiple Solvent Crystal Structures (MSCS)[27] and Structure–Activity Relationship by Nuclear Magnetic Resonance (SAR by NMR).[28] MSCS determines the X-ray structures of a target protein in aqueous solutions containing high concentrations of organic co-solvents and then superimposes the obtained crystal structures. Consensus binding sites have been observed from these crystal structures. A consensus binding site typically accommodates a number of different organic probes binding in well-defined orientations. SAR by NMR screens a library of fragments using NMR and identifies the specific binding pocket for each fragment hit, guiding the synthesis of larger molecules from the fragments that bind at multiple binding sites (Fig. 4). A fragment here is defined as a small organic molecule that follows the "rule of three" [29] (the molecular weight of the compound $\leqslant$300, *Clog*P $\leqslant$3, the number of H-bond donors $\leqslant$3, the number of H-bond acceptors $\leqslant$3, the number of rotatable bonds $\leqslant$3, and polar surface area (PSA) $\leqslant$60 Å^2). The SAR by NMR studies observed the existence of consensus binding sites at protein–protein interfaces. Further studies of MSCS and SAR by NMR demonstrated that these consensus binding sites were often overlapped with energetic hot regions discovered through alanine scanning. Starting on a different path, protein phage display studies demonstrated that short peptides with entirely different structural scaffolds bound to the concave hot region and mimicked the binding mode for native PPIs.[30] These observations provide strong support for the efforts to discover small-molecule PPI inhibitors.

One should bear in mind that in identifying hot spots, alanine scanning experiments examine the contributions to the mutual interaction energy between two proteins, investigating both the concave and convex PPI regions. In contrast, the 'consensus binding site' derived from MSCS or SAR by NMR is a property of a single protein, usually the concave PPI surface.[31] The energetically favored region identified by fragment screening is not necessarily a PPI hot region as its binding is determined simply by the concavity of the surface pocket and the chemical complementary with fragment probes. If the structure of the protein–protein complex and the protruding hot spots are known, the relationship between the consensus binding sites identified by fragment screening and the concave hot regions can be established. FTMap, a computational solvent mapping program based on the fast Fourier transform correlation approach, has been used to predict the consensus binding site for 16 common solvents/small organic molecules.[32] The mapping results of FTMap have a high agreement with those derived from the X-ray crystallography and NMR studies.[31,33] FTMap is also able to rank the relative importance of the identified consensus binding sites.

Inspired by the results of MSCS, SAR by NMR, and computational solvent mapping, fragment screening has been used to identify new hits for PPI targets.[34] The libraries for fragment screening

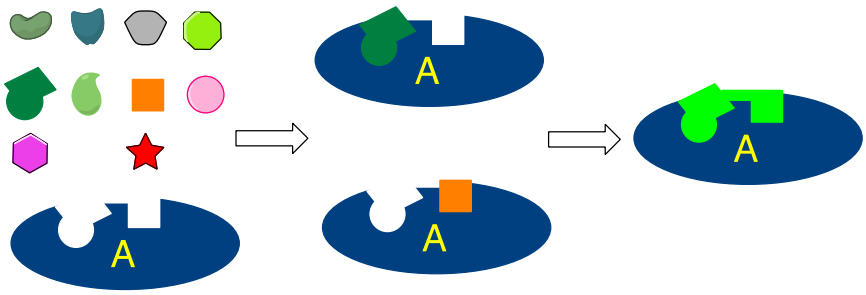

Figure 4. Schematic diagram for SAR by NMR. The binding modes of a collection of fragments with target protein are studied by two-dimensional NMR spectra. The fragment hits from the NMR-based screen are then linked or evolved into drug-like molecules.

contain hundreds to thousands of low-molecular-weight fragments, which are screened at high concentrations. The binding affinities of commercially available fragments to protein targets are typically low. Highly sensitive biophysical methods are required to identify the fragments with weak binding affinities. The common techniques for fragment screening include NMR, X-ray crystallography, cysteine engineering-based tethering,[35,36] surface plasmon resonance (SPR), thermal shift[37] and confocal fluorescence correlation spectroscopy-based[38] assays. These methods can also be used in a synergistic way.[39] Dozens of potent PPI inhibitors with novel scaffolds have been reported by use of fragment screening coupled with structure-based optimization. Some well-known examples are the inhibitors for anti-apoptotic protein BCL-X_L/pro-apoptotic protein BAK interactions (Fig. 5A),[40] tumor necrosis factor α (TNF-α)/tumor necrosis factor receptor 1 (TNFR1) interactions,[41] and interleukin-2 (IL-2)/interleukin-2α receptor (IL-2Rα) interactions.[36] It is worth noting that without structural and biochemical validation the fragments identified by fragment screening are not always useful for developing PPI inhibitors. If a fragment binds to the protein pocket outside the hot region, it may have no use. Carelessly evolving a fragment hit or linking two fragment hits might lead to a small molecule that tightly binds to the target protein but has no effect on disrupting PPIs. The prior knowledge of hot spots and hot regions derived from biochemical and crystallographic studies is essential for the success of fragment screening. An alternative to experimental fragment screening is hot spot-based virtual screening using a database of fragment-size molecules. One example is the discovery of **4** in Figure 5B as an inhibitor for interferon-α (IFN-α)/type I interferon receptor (IFNAR) interactions.[42] NMR and SPR experiments confirm the direct binding of **4** with IFN-α.

The characteristics of a druggable PPI hot region have been investigated.[48,49] The druggability of a pocket increases logarithmically with total surface area and apolar contact area, while it decreases logarithmically with polar contact area. The polar groups in the druggable binding site play a decisive role in recognizing drug-like small molecules.[50] There is an optimal size and composition of a protein pocket that is best suited for interacting with small organic molecules. The druggability of a protein pocket increases linearly with surface roughness.[51] Pocket shape also has a significant influence on druggability. The optimal value for pocket compactness (defined as pocket volume divided by pocket surface area) is ~0.4. Large values, corresponding to more spherical shapes, or small values, corresponding to more elongated shapes, have a decreased contribution towards druggability. The amino acid composition around druggable PPI pockets is markedly different from that in the other areas on the protein surface. A higher frequency of aromatic residues and methionine has been observed in druggable PPI pockets.[52] The molecular interplay between amino acids at a given hot region is also worth attention when identifying druggable PPI pockets. An increasing number of charged residues was reported to have a negative impact on the druggability of a pocket.[48] Furthermore, the conformational fluctuations of the areas adjacent to hot regions due to inherent thermal motions of a protein could open up transient pockets[53] that are important for accommodating a PPI inhibitor with drug-like dimensions.[54] It was reported that druggable sites on PPIs are more predisposed than the rest of protein surface and more likely to accommodate drug-like molecules.[55] Indeed, mapping surface pockets by FTMap with a side-chain conformer generator successfully identified druggable sites in the protein–protein interfaces.[56]

Case study 1: Due to the facts that: (1) the hot regions of PPIs are pre-organized on the protein surface and complementarily packed between two proteins; (2) the hot spots in the concave hot regions are deeply buried; and (3) the conformational transition to open up a new pocket for drug-like inhibitors has little energetic cost, it is arguable that hot spot-based design could be an efficient approach in discovering drug-like PPI inhibitors. Wang and co-workers have used hot spot-based design to discover a series of spirooxindole-containing inhibitors for murine double minute 2 (MDM2)/tumor suppressor p53 interactions (Fig. 6). The inhibition of MDM2/p53 interactions by small molecules can restore the level of wild-type p53 and represents an appealing strategy for anticancer therapy. Crystallographic and biochemical studies revealed that three hydrophobic residues, F19, W23, and L26 from an α-helix in p53, form a hot region to interact with a concave hydrophobic hot region in MDM2. The indole ring of p53 W23 was used as the starting point for inhibitor design, and the spirooxindole structure was used to build the inhibitor scaffold.[57] The oxindole moiety of the spirooxindole core was designed to mimic the binding mode of the side chain of p53 W23. Two hydrophobic substituents on the spirooxindole core, R^1 and R^2, were designed to mimic the binding mode of the side chains of F19 and L26, respectively. After the synthesis, compound **5** was found to have a K_i value of 0.086 ± 0.02 μM for disrupting MDM2/p53 PPIs. The optimization resulted in the discovery of MI-63 with a K_i value of 0.003 ± 0.0015 μM.[58] Consistent with its mode of action, MI-63 inhibits the growth of cancer cells with wild-type p53. Derivation to increase oral bioavailability and in vivo activity led to MI-219[59] and MI-888.[60] MI-888 exhibits a K_i value of 0.00044 ± 0.00022 μM for disrupting MDM2/p53 interactions. This compound induces tumor regression in two xenograft models in a complete and durable manner.

Case study 2: Dömling, Camacho, and co-workers also performed hot spot-based design to discover MDM2/p53 PPI inhibitors (Fig. 7). Residue W23 of p53 was again used as the starting point to initiate the design. 6-Chloroindole and 4-chlorobenzene were defined as anchor fragments to mimic the indole ring of p53 W23. Multicomponent reactions (MCRs) were used to produce diverse scaffolds containing the 6-chloroindolyl or 4-chlorophenyl group.[61] The van Leusen three-component reaction was used to synthesize WK23, which exhibited a K_i value of 0.916 μM. The crystallographic analysis of MDM2 in complex with WK23 demonstrated that the

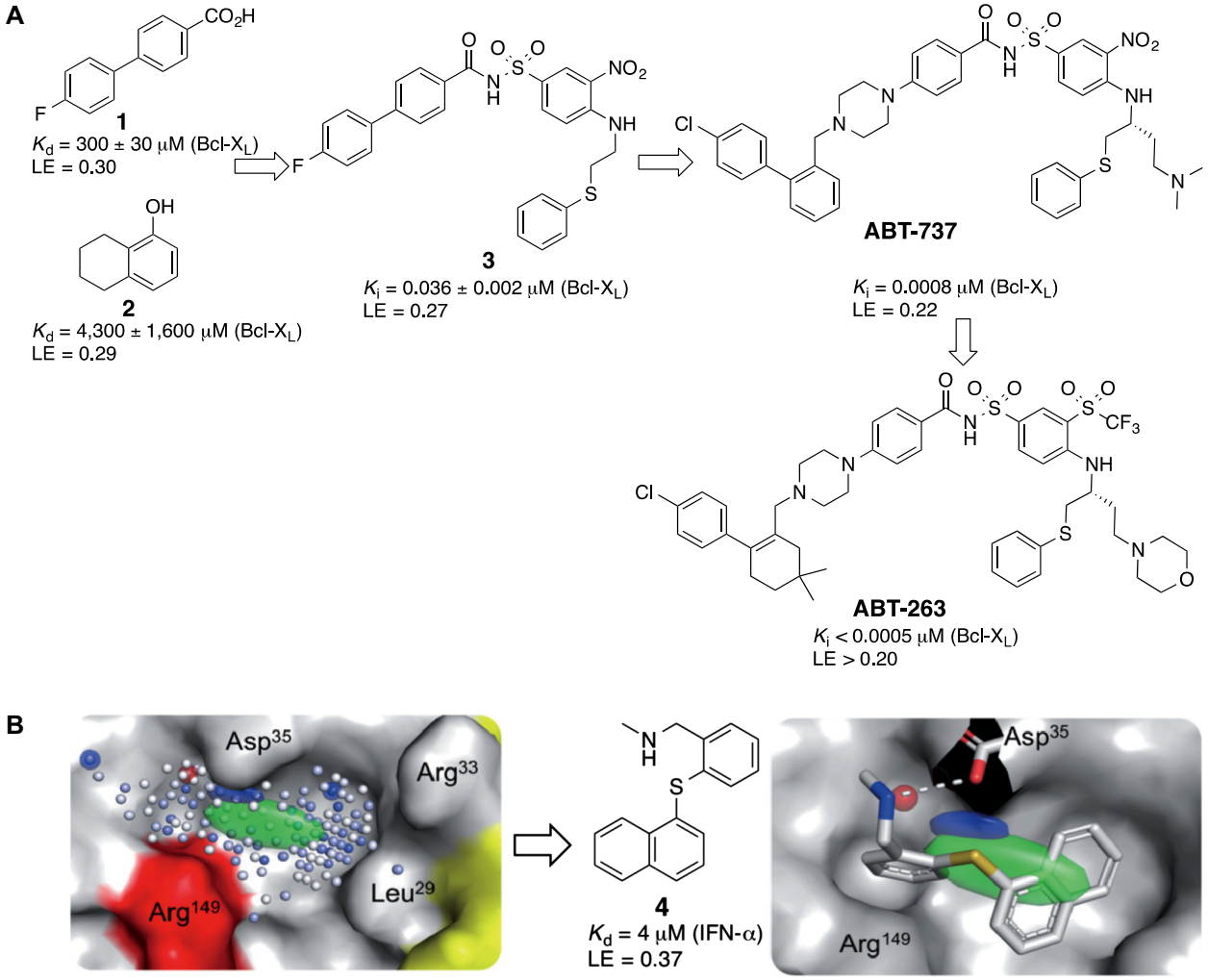

Figure 5. Fragment-based screen to discover PPI inhibitors. (A) The discovery of BCL-X_L/BAK inhibitors. Fragments **1** and **2** were identified by SAR by NMR. They bind at two proximal subpockets on the BCL-X_L surface. Medicinal chemistry optimization yielded **3** with a K_i value of 0.036 ± 0.002 μM for disrupting BCL-X_L/BAK interactions.[43] Subsequent lead optimization aimed at removing the binding to human serum albumin[44] and increasing potency to other BCL family proteins,[45] which led to ABT-737.[40] Further optimization was centered to improve oral pharmacokinetics and resulted in the discovery of ABT-263.[46] (B) Hot spot-based virtual screening identified **4** as an inhibitor for IFN-α/IFNAR interactions.[42] Pharmacophore model (green, lipophilic center; blue, hydrogen-bond donor; red, hydrogen-bond acceptor) inside the binding pocket of INF-α and a docking pose of **4** in IFN-α were provided. LE, ligand efficiency; it is defined as free energy of ligand binding ($\Delta\Delta G = -RT\ln K_d$ or $\Delta\Delta G = -RT\ln K_i$, R: gas constant, T, Kelvin temperature used in the assays) divided by the number of non-hydrogen atoms of the tested compound.[47]

6-chloroindole moiety of WK23 was located at the same position as the side chain of p53 W23. The 6-chlorine atom of WK23 is positioned towards the very bottom of this concave hot region.[62] The nitrogen atom of 6-chloroindole forms a hydrogen bond with L54 carbonyl oxygen of MDM2 and mimics the binding mode of the indole nitrogen of p53 W23. The 4-chlorobenzyl group and the phenyl rings of WK23 occupy the L26 and F19 binding sites of p53, respectively. Further modification of the WK23 structure led to the generation of WK298 exhibiting a K_i value of 0.109 μM. The Ugi four-component reaction was used to generate KK271[63], YH239[64], and **6**[65], which had K_i values of 1.2, 0.4, and 0.25 μM, respectively. A crystallographic analysis revealed a conformational change of the aromatic residues around the p53 F19/W23/L26 binding site.[66] The 4-chlorobenzyl group was introduced to YH119 to generate YH300 with a K_i value of 0.6 μM.

Case study 3: Crews, Ciulli, and co-workers designed inhibitors for von Hippel-Lindau (VHL)/hypoxia-inducible factor 1α (HIF1α) interactions (Fig. 8).[67] The VHL protein is a component of the E3 ligase. The formation of the VHL/HIF1α complex promotes the ubiquitination and degradation of HIF1α by the proteasome. The accumulation of HIF1α upregulates the genes that are involved in hypoxic response, and VHL/HIF1α inhibitors can potentially be used to treat chronic anemia. 3-Hydroxyl-L-proline (Hyp) 564 of HIF1α is a hot spot for interacting with VHL. This residue was used as a starting point to design new inhibitors with the assistance of *de novo* design software BOMB.[68] Compound **8** was discovered to exhibit an IC_{50} value of 117 ± 10 μM. The isoxazole moiety of **8** was designed to interact with a crystallographic water observed in the VHL/HIF1α complex. The benzyl group of **8** was designed to stack with the side chain of Y98. An oxazole ring was then introduced to the *para* position of the benzyl group, resulting in **9** with an IC_{50} value of 4.1 ± 0.4 μM. Crystallographic analysis showed that the nitrogen atom of the oxazole ring formed an H-bond with R107 of VHL, and the C–H at position 2 of the oxazole ring in **9** formed a nonclassical H-bond with the carboxyl oxygen of P99. Further optimization led to the generation of **10**. In this compound the 4-methylthiazole ring replaced the oxazole ring, resulting in better interactions with a hydrophobic pocket in VHL. A substituted aniline was used to replace the isoxazolmethyl moiety. Crystallographic analysis showed that the aniline ring lay adjacent to the side chain of W88 and made a water-mediated H-bond with Q96 of VHL. This compound exhibited improved potency, with an IC_{50} value of 0.90 ± 0.03 μM.[69]

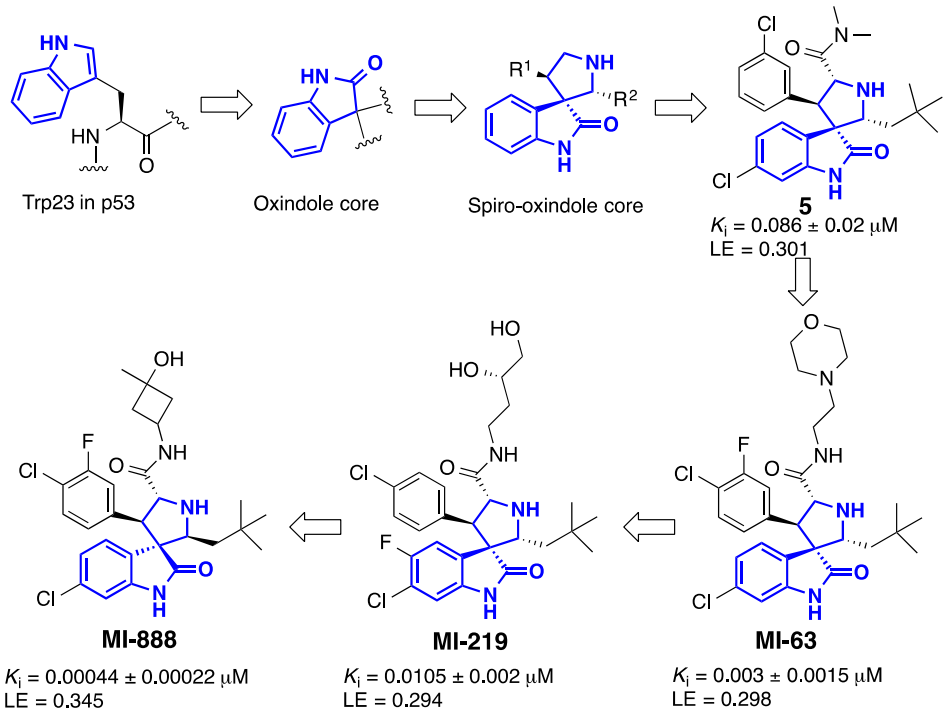

Figure 6. Hot spot-based design of spirooxindole-containing MDM2/p53 PPI inhibitors. LE, ligand efficiency.

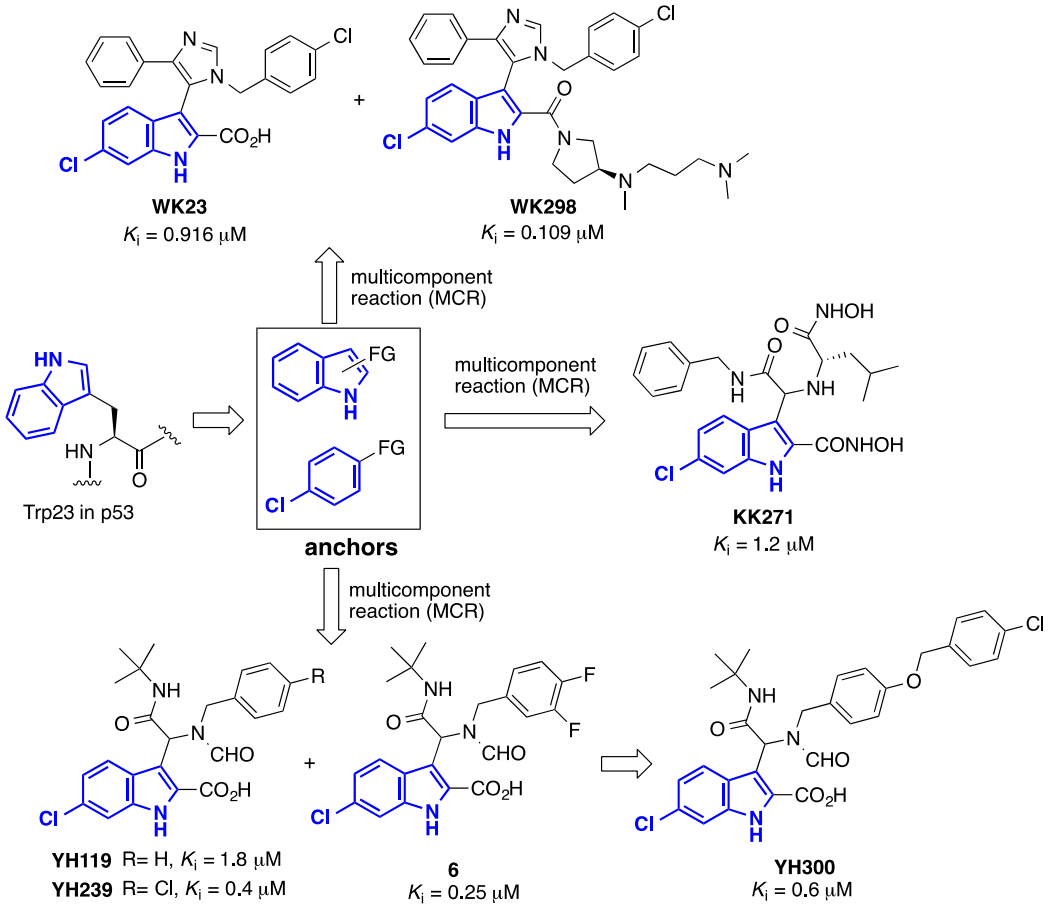

Figure 7. Anchor-oriented design of chloroindole-containing MDM2/p53 PPI inhibitors.

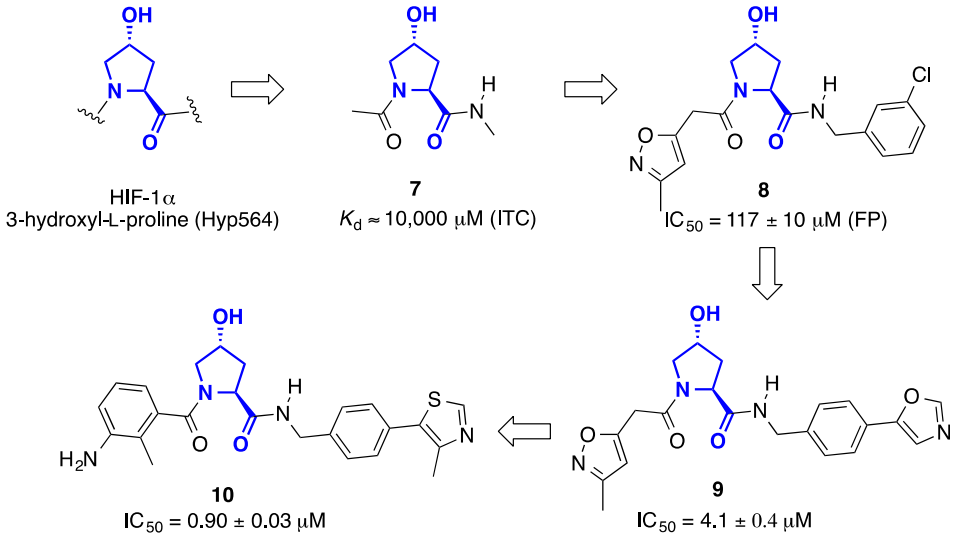

Figure 8. Hot spot-based design of hydroxyproline-containing VHL/HIF1α PPI inhibitors.

Case study 4: Ji and coworkers used fragment hopping[70] to initiate the design of potent and selective PPI inhibitors. Fragment hopping requires the extraction of key binding elements based on the binding mode between the projecting hot spots and the concave hot spot pocket. The bioisosteric replacement technique is then used to design new fragments that match the proposed critical binding elements and generate new inhibitor structures with the chemotypes that do not exist in hot spots. As the first case study for PPI targets, this approach was employed to design potent and selective inhibitors for β-catenin/T-cell factor (Tcf) interactions (Fig. 9).[71] The β-catenin/Tcf protein–protein complex is a key downstream effector of the canonical Wnt signaling pathway. The aberrant formation of this protein–protein complex overactivates Wnt target genes that cause the initiation and progression of many cancers and fibroses. The previous crystallographic and biochemical studies revealed three hot regions for β-catenin/Tcf PPIs, as shown in Figure 1. The contribution of each hot region was quantitatively evaluated, and the D16/K435 and E17/K508 interactions were identified essential for the formation of the β-catenin/Tcf complex. Bioisosteres were used to mimic the binding mode of side chain carboxylic acids of Tcf4 D16 and E17, which led to UU-T01 with a K_i value of 3.14 ± 0.48 μM. This compound completely disrupts β-catenin/Tcf interactions and is two orders of magnitude more potent than dipeptide D–E. The binding mode of the designed inhibitors was evaluated by site-directed mutagenesis and structure–activity relationship (SAR) studies. Further synthesis resulted in the discovery of **11** with a K_i value of 1.35 ± 0.15 μM (unpublished result, Ji et al.) From a different direction, residues D16 and E17 of human Tcf4 were maintained in the inhibitor scaffold. SiteMap[72] and Multiple-Copy Simultaneous Search (MCSS)[73] were used to map the pockets adjacent to K435 and K508. Based on the structure of Tcf4 peptide G[13]ANDE[17], a peptidomimetic strategy was used to design new inhibitors. Compound **12** was discovered with a K_i value of 1.36 ± 0.12 μM.[74] The binding mode of **12** was also evaluated by site-directed mutagenesis and SAR studies. The ethyl ester derivative of **12** can effectively penetrate the cell membrane and inhibit canonical Wnt signaling and the growth of colorectal cancer cells. This compound also exhibits cell-based selectivities for β-catenin/Tcf over β-catenin/cadherin and β-catenin/adenomatous polysis coli (APC) interactions. A further application of fragment hopping to scaffolds **11** and **12** led to the generation of new inhibitors with nanomolar inhibitory potency for β-catenin/Tcf interactions and high selectivity for β-catenin/Tcf over β-catenin/cadherin and β-catenin/APC interactions (unpublished results, Ji et al.)

Conclusion and outlook: The discovery of small-molecule PPI inhibitors has been difficult. The low success rate for discovering PPI inhibitors was primarily ascribed to: (1) the overall characteristic of the protein–protein interface, which is large, flat, and featureless. The amount of buried surface area upon the formation of the protein–protein complex greatly exceeds the potential binding area of a small molecule, which highlights the value of rational design of PPI inhibitors and the need for new techniques to detect transient pockets; (2) the compound libraries used in HTS and virtual screening. The currently available compound collections were traditionally synthesized for enzyme and receptor targets, which

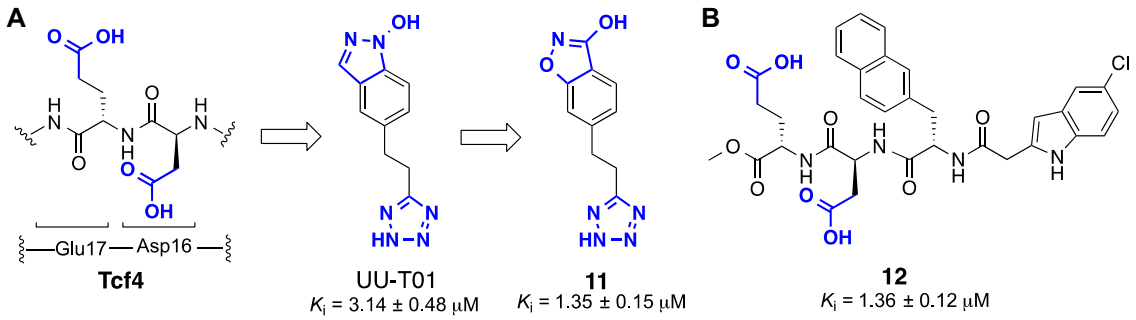

Figure 9. Hot spot-based design of β-catenin/T-cell factor PPI inhibitors. (A) Bioisoteric replacement technique to design UU-T01 and **11**. (B) Peptidomimetic strategy to design **12**.

contain binding sites drastically different from those in the protein–protein surfaces. The compound survey studies indicate that PPI inhibitors tend to be larger, more hydrophobic, more rigid, and contain multiple aromatic rings;[75] (3) the difficulty to attain reliable HTS assays for some PPI targets, in particular for the weak PPIs with large contact surfaces;[76] and (4) the flexibility of the protein surface around hot regions, which accounts for some failures of virtual screening. Hot spot-based design of PPI inhibitors is a valuable strategy for discovering PPI inhibitors. The hot spots and hot regions of PPIs can be identified and quantitatively evaluated by biochemical and crystallographic studies. Biologically important and druggable concave hot regions can be identified from the protein–protein interface. Sometimes, energetic cooperativity exists between two hot regions. The potency of a PPI inhibitor that targets a cooperative hot region can be amplified relative to the inhibitor that targets a hot region that is strictly additive. Fragment-size inhibitors can be designed and synthesized to mimic the binding mode of hot spots in a specified hot region that contributes most to the free energy of binding. Fragment hopping can play an important role in designing such anchor fragments with new chemotypes. An O-ring structure can further be built into inhibitor structures to complement the concave hot region of PPIs when enlarging an anchor fragment.

Protein adaptability has frequently been observed for the structures around the hot regions of PPIs. Taking into account protein adaptability in the process of generating drug-like PPI inhibitors is critical; this is also the advantage of hot spot-based design. After the design and validation of an anchor fragment for one concave hot region, this anchor fragment can be evolved into a drug-like PPI inhibitor with the consideration of protein adaptability.

Cellular proteins often use the same surface to bind with a structurally diverse set of proteins in different organelles or cellular environments. Inside of the cell, there is a complex network of PPIs.[77] With the mapping of the drug-target network,[78] the evaluation and leverage of the selectivity/specificity of PPI inhibitors has become an emerging field. Hot spot-based design matches well with the need to discover PPI inhibitors with high selectivity/specificity because the hot spots that are essential for different binding partners could be located in different hot regions when more than one hot region exists on the protein surface.[9] For the proteins that use one identical hot region for interacting with multiple protein partners the key binding elements for PPI selectivity often reside in the protein–protein interface adjacent to the concave hot region.[74,79] Indeed, hot spot-based inhibitor design for PPI target is still at its beginning stage, and few examples have been reported. More techniques need to be developed, and a surge of research in this field can be expected in the coming years.

References and notes

1. Lo Conte, L.; Chothia, C.; Janin, J. *J. Mol. Biol.* **1999**, *285*, 2177.
2. Arkin, M. R.; Wells, J. A. *Nat. Rev. Drug Disc.* **2004**, *3*, 301.
3. Wells, J. A.; McClendon, C. L. *Nature* **2007**, *450*, 1001.
4. Keskin, O.; Gursoy, A.; Ma, B.; Nussinov, R. *Chem. Rev.* **2008**, *108*, 1225.
5. Clackson, T.; Wells, J. A. *Science* **1995**, *267*, 383.
6. Bogan, A. A.; Thorn, K. S. *J. Mol. Biol.* **1998**, *280*, 1.
7. Hu, Z.; Ma, B.; Wolfson, H.; Nussinov, R. *Proteins* **2000**, *39*, 331.
8. Ma, B.; Elkayam, T.; Wolfson, H.; Nussinov, R. *Proc. Natl. Acad. Sci. U.S.A.* **2003**, *100*, 5772.
9. Carbonell, P.; Nussinov, R.; del Sol, A. *Proteomics* **2009**, *9*, 1744.
10. Keskin, O.; Ma, B.; Nussinov, R. *J. Mol. Biol.* **2005**, *345*, 1281.
11. Reichmann, D.; Rahat, O.; Albeck, S.; Meged, R.; Dym, O.; Schreiber, G. *Proc. Natl. Acad. Sci. U.S.A.* **2005**, *102*, 57.
12. Moza, B.; Buonpane, R. A.; Zhu, P.; Herfst, C. A.; Rahman, A. K. M. N.-u.; McCormick, J. K.; Kranz, D. M.; Sundberg, E. J. *Proc. Natl. Acad. Sci. U.S.A.* **2006**, *103*, 9867.
13. Golden, M. S.; Cote, S. M.; Sayeg, M.; Zerbe, B. S.; Villar, E. A.; Beglov, D.; Sazinsky, S. L.; Georgiadis, R. M.; Vajda, S.; Kozakov, D.; Whitty, A. *J. Am. Chem. Soc.* **2013**, *135*, 6242.
14. Rajamani, D.; Thiel, S.; Vajda, S.; Camacho, C. J. *Proc. Natl. Acad. Sci. U.S.A.* **2004**, *101*, 11287.
15. Meireles, L. M. C.; Dömling, A. S.; Camacho, C. J. *Nucleic Acids Res.* **2010**, *38*, W407.
16. Li, X.; Keskin, O.; Ma, B.; Nussinov, R.; Liang, J. *J. Mol. Biol.* **2004**, *344*, 781.
17. Morrow, J. K.; Zhang, S. *Curr. Pharm. Des.* **2012**, *18*, 1255.
18. Kortemme, T.; Baker, D. *Proc. Natl. Acad. Sci. U.S.A.* **2002**, *99*, 14116.
19. Guerois, R.; Nielsen, J. E.; Serrano, L. *J. Mol. Biol.* **2002**, *320*, 369.
20. (a) Massova, I.; Kollman, P. A. *J. Am. Chem. Soc.* **1999**, *121*, 8133; (b) Moreira, I. S.; Fernandes, P. A.; Ramos, M. J. *J. Comput. Chem.* **2007**, *28*, 644.
21. (a) Darnell, S. J.; LeGault, L.; Mitchell, J. C. *Nucleic Acids Res.* **2008**, *36*, W265; (b) Tuncbag, N.; Gursoy, A.; Keskin, O. *Bioinformatics* **2009**, *25*, 1513; (c) Cho, K.-I.; Kim, D.; Lee, D. *Nucleic Acids Res.* **2009**, *37*, 2672; (d) Xia, J.-F.; Zhao, X.-M.; Song, J.; Huang, D.-S. *BMC Bioinformatics* **2010**, *11*, 174; (e) Zhu, X.; Mitchell, J. C. *Proteins* **2011**, *79*, 2671.
22. (a) Masso, M.; Vaisman, I. I. *Bioinformatics* **2002**, *2008*, 24; (b) Lise, S.; Archambeau, C.; Pontil, M.; Jones, D. T. *BMC Bioinformatics* **2009**, *10*, 365.
23. (a) Li, J.; Liu, Q. *Bioinformatics* **2009**, *25*, 743; (b) Liu, Q.; Li, J. *BMC Bioinformatics* **2010**, *11*, 244.
24. (a) Moreira, I. S.; Fernandes, P. A.; Ramos, M. J. *J. Phys. Chem. B* **2007**, *111*, 2697; (b) Moreira, I. S.; Ramos, R. M.; Martins, J. M.; Fernandes, P. A.; Ramos, M. J. *J. Biomol. Struct. Dyn.* **2014**, *32*, 186.
25. Li, Z.; Li, J. *Proteins* **2010**, *78*, 3304.
26. Fuller, J. C.; Burgoyne, N. J.; Jackson, R. M. *Drug Discovery Today* **2009**, *14*, 155.
27. Mattos, C.; Ringe, D. *Nat. Biotechnol.* **1996**, *14*, 595.
28. Shuker, S. B.; Hajduk, P. J.; Meadows, R. P.; Fesik, S. W. *Science* **1996**, *274*, 1531.
29. Congreve, M.; Carr, R.; Murray, C.; Jhoti, H. *Drug Discovery Today* **2003**, *8*, 876.
30. DeLano, W. L.; Ultsch, M. H.; de Vos, A. M.; Wells, J. A. *Science* **2000**, *287*, 1279.
31. Zerbe, B. S.; Hall, D. R.; Vajda, S.; Whitty, A.; Kozakov, D. *J. Chem. Inf. Model.* **2012**, *52*, 2236.
32. Brenke, R.; Kozakov, D.; Chuang, G.-Y.; Beglov, D.; Hall, D.; Landon, M. R.; Mattos, C.; Vajda, S. *Bioinformatics* **2009**, *25*, 621.
33. (a) Buhrman, G.; O'Connor, C.; Zerbe, B.; Kearney, B. M.; Napoleon, R.; Kovrigina, E. A.; Vajda, S.; Kozakov, D.; Kovrigin, E. L.; Mattos, C. *J. Mol. Biol.* **2011**, *413*, 773; (b) Hall, D. H.; Grove, L. E.; Yueh, C.; Ngan, C. H.; Kozakov, D.; Vajda, S. *J. Am. Chem. Soc.* **2011**, *133*, 20668.
34. Winter, A.; Higueruelo, A. P.; Marsh, M.; Sigurdardottir, A.; Pitt, W. R.; Blundell, T. L. Q. *Rev. Biophys.* **2012**, *45*, 383.
35. Erlanson, D. A.; Braisted, A. C.; Raphael, D. R.; Randal, M.; Stroud, R. M.; Gordon, E. M.; Wells, J. A. *Proc. Natl. Acad. Sci. U.S.A.* **2000**, *97*, 9367.
36. Braisted, A. C.; Oslob, J. D.; Delano, W. L.; Hyde, J.; McDowell, R. S.; Waal, N.; Yu, C.; Arkin, M. R.; Raimundo, B. C. *J. Am. Chem. Soc.* **2003**, *125*, 3714.
37. Scott, D. E.; Ehebauer, M. T.; Pukala, T.; Marsh, M.; Blundell, T. L.; Venkitaraman, A. R.; Abell, C.; Hyvönen, M. *ChemBioChem* **2013**, *14*, 332.
38. Mikuni, J.; Kato, M.; Taruya, S.; Tsuganezawa, K.; Mori, M.; Ogawa, N.; Honma, T.; Yokoyama, S.; Kojima, H.; Okabe, T.; Nagano, T.; Tanaka, A. *Anal. Biochem.* **2010**, *402*, 26.
39. Davis, B. J.; Erlanson, D. A. *Bioorg. Med. Chem. Lett.* **2013**, *23*, 2844.
40. Oltersdorf, T.; Elmore, S. W.; Shoemaker, A. R.; Armstrong, R. C.; Augeri, D. J.; Belli, B. A.; Bruncko, M.; Deckwerth, T. L.; Dinges, J.; Hajduk, P. J.; Joseph, M. K.; Kitada, S.; Korsmeyer, S. J.; Kunzer, A. R.; Letai, A.; Li, C.; Mitten, M. J.; Nettesheim, D. G.; Ng, S.; Nimmer, P. M.; O'Connor, J. M.; Oleksijew, A.; Petros, A. M.; Reed, J. C.; Shen, W.; Tahir, S. K.; Thompson, C. B.; Tomaselli, K. J.; Wang, B.; Wendt, M. D.; Zhang, H.; Fesik, S. W.; Rosenberg, S. H. *Nature* **2005**, *435*, 677.
41. He, M. M.; Smith, A. S.; Oslob, J. D.; Flanagan, W. M.; Braisted, A. C.; Whitty, A.; Cancilla, M. T.; Wang, J.; Lugovskoy, A. A.; Yoburn, J. C.; Fung, A. D.; Farrington, G.; Eldredge, J. K.; Day, E. S.; Cruz, L. A.; Cachero, T. G.; Miller, S. K.; Friedman, J. E.; Choong, I. C.; Cunningham, B. C. *Science* **2005**, *310*, 1022.
42. Geppert, T.; Bauer, S.; Hiss, J. A.; Conrad, E.; Reutlinger, M.; Schneider, P.; Weisel, M.; Pfeiffer, B.; Altmann, K.-H.; Waibler, Z.; Schneider, G. *Angew. Chem., Int. Ed.* **2012**, *51*, 258.
43. Petros, A. M.; Dinges, J.; Augeri, D. J.; Baumeister, S. A.; Betebenner, D. A.; Bures, M. G.; Elmore, S. W.; Hajduk, P. J.; Joseph, M. K.; Landis, S. K.; Nettesheim, D. G.; Rosenberg, S. H.; Shen, W.; Thomas, S.; Wang, X.; Zanze, I.; Zhang, H.; Fesik, S. W. *J. Med. Chem.* **2006**, *49*, 656.
44. Wendt, M. D.; Shen, W.; Kunzer, A.; McClellan, W. J.; Bruncko, M.; Oost, T. K.; Ding, H.; Joseph, M. K.; Zhang, H.; Nimmer, P. M.; Ng, S.-C.; Shoemaker, A. R.; Petros, A. M.; Oleksijew, A.; Marsh, K.; Bauch, J.; Oltersdorf, T.; Belli, B. A.; Martineau, D.; Fesik, S. W.; Rosenberg, S. H.; Elmore, S. W. *J. Med. Chem.* **2006**, *49*, 1165.
45. Bruncko, M.; Oost, T. K.; Belli, B. A.; Ding, H.; Joseph, M. K.; Kunzer, A.; Martineau, D.; McClellan, W. J.; Mitten, M.; Ng, S.-C.; Nimmer, P. M.; Oltersdorf, T.; Park, C.-M.; Petros, A. M.; Shoemaker, A. R.; Song, X.; Wang, X.; Wendt, M. D.; Zhang, H.; Fesik, S. W.; Rosenberg, S. H.; Elmore, S. W. *J. Med. Chem.* **2007**, *50*, 641.
46. Park, C.-M.; Bruncko, M.; Adickes, J.; Bauch, J.; Ding, H.; Kunzer, A.; Marsh, K. C.; Nimmer, P.; Shoemaker, A. R.; Song, X.; Tahir, S. K.; Tse, C.; Wang, X.; Wendt, M. D.; Yang, X.; Zhang, H.; Fesik, S. W.; Rosenberg, S. H.; Elmore, S. W. *J. Med. Chem.* **2008**, *51*, 6902.
47. Hopkins, A. L.; Groom, C. R.; Alex, A. *Drug Discovery Today* **2004**, *9*, 430.
48. Hajduk, P. J.; Huth, J. R.; Fesik, S. W. *J. Med. Chem.* **2005**, *48*, 2518.
49. Cheng, A. C.; Coleman, R. G.; Smyth, K. T.; Cao, Q.; Soulard, P.; Caffrey, D. R.; Salzberg, A. C.; Huang, E. S. *Nat. Biotechnol.* **2007**, *25*, 71.
50. Schmidtke, P.; Barril, X. *J. Med. Chem.* **2010**, *53*, 5858.
51. Pettit, F. K.; Bowie, J. U. *J. Mol. Biol.* **1999**, *285*, 1377.
52. (a) Soga, S.; Shirai, H.; Kobori, M.; Hirayama, N. *J. Chem. Inf. Model.* **2007**, *47*, 400; (b) Li, Y.; Liu, Z.; Han, L.; Li, C.; Wang, R. *J. Chem. Inf. Model.* **2013**, *53*, 2437.

53. Metz, A.; Pfleger, C.; Kopitz, H.; Pfeiffer-Marek, S.; Baringhaus, K.-H.; Gohlke, H. *J. Chem. Inf. Model.* **2012**, *52*, 120.
54. Eyrisch, S.; Helms, V. *J. Med. Chem.* **2007**, *50*, 3457.
55. Johnson, D. K.; Karanicolas, J. *PLoS Comput. Biol.* **2013**, *9*, e1002951.
56. Kozakov, D.; Hall, D. R.; Chuang, G.-Y.; Cencic, R.; Brenke, R.; Grove, L. E.; Beglov, D.; Pelletier, J.; Whitty, A.; Vajda, S. *Proc. Natl. Acad. Sci. U.S.A.* **2011**, *108*, 13528.
57. Ding, K.; Lu, Y.; Nikolovska-Coleska, Z.; Qiu, S.; Ding, Y.; Gao, W.; Stuckey, J.; Krajewski, K.; Roller, P. P.; Tomita, Y.; Parrish, D. A.; Deschamps, J. R.; Wang, S. *J. Am. Chem. Soc.* **2005**, *127*, 10130.
58. Ding, K.; Lu, Y.; Nikolovska-Coleska, Z.; Wang, G.; Qiu, S.; Shangary, S.; Gao, W.; Qin, D.; Stuckey, J.; Krajewski, K.; Roller, P. P.; Wang, S. *J. Med. Chem.* **2006**, *49*, 3432.
59. Shangary, S.; Qin, D.; McEachern, D.; Liu, M.; Miller, R. S.; Qiu, S.; Nikolovska-Coleska, Z.; Ding, K.; Wang, G.; Chen, J.; Bernard, D.; Zhang, J.; Lu, Y.; Gu, Q.; Shah, R. B.; Pienta, K. J.; Ling, X.; Kang, S.; Guo, M.; Sun, Y.; Yang, D.; Wang, S. *Proc. Natl. Acad. Sci. U.S.A.* **2008**, *105*, 3933.
60. (a) Zhao, Y.; Liu, L.; Sun, W.; Lu, J.; McEachern, D.; Li, X.; Yu, S.; Bernard, D.; Ochsenbein, P.; Ferey, V.; Carry, J.-C.; Deschamps, J. R.; Sun, D.; Wang, S. *J. Am. Chem. Soc.* **2013**, *135*, 7223; (b) Zhao, Y.; Yu, S.; Sun, W.; Liu, L.; Lu, J.; McEachern, D.; Shargary, S.; Bernard, D.; Li, X.; Zhao, T.; Zou, P.; Sun, D.; Wang, S. *J. Med. Chem.* **2013**, *56*, 5553.
61. Czarna, A.; Beck, B.; Srivastava, S.; Popowicz, G. M.; Wolf, S.; Huang, Y.; Bista, M.; Holak, T. A.; Dömling, A. *Angew. Chem., Int. Ed.* **2010**, *49*, 5352.
62. Popowicz, G. M.; Czarna, A.; Wolf, S.; Wang, K.; Wang, W.; Dömling, A.; Holak, T. A. *Cell Cycle* **2010**, *9*, 1104.
63. Koes, D.; Khoury, K.; Huang, Y.; Wang, W.; Bista, M.; Popowicz, G. M.; Wolf, S.; Holak, T. A.; Dömling, A.; Camacho, C. J. *PLoS ONE* **2012**, *7*, e32839.
64. Huang, Y.; Wolf, S.; Beck, B.; Köhler, L.-M.; Khoury, K.; Popowicz, G. M.; Goda, S. K.; Subklewe, M.; Twarda, A.; Holak, T. A.; Dömling, A. *ACS Chem. Biol.* **2014**, *9*, 802.
65. Huang, Y.; Wolf, S.; Koes, D.; Popowicz, G. M.; Camacho, C. J.; Holak, T. A.; Dömling, A. *ChemMedChem* **2012**, *7*, 49.
66. Bista, M.; Wolf, S.; Khoury, K.; Kowalska, K.; Huang, Y.; Wrona, E.; Arciniega, M.; Popowicz, G. M.; Holak, T. A.; Dömling, A. *Structure* **2013**, *21*, 2143.
67. (a) Buckley, D. L.; Van Molle, I.; Gareiss, P. C.; Tae, H. S.; Michel, J.; Noblin, D. J.; Jorgensen, W. L.; Ciulli, A.; Crews, C. M. *J. Am. Chem. Soc.* **2012**, *134*, 4465; (b) Van Molle, I.; Thomann, A.; Buckley, D. L.; So, E. C.; Lang, S.; Crews, C. M.; Ciulli, A. *Chem. Biol.* **2012**, *19*, 1300.
68. Jorgensen, W. L. *Acc. Chem. Res.* **2009**, *42*, 724.
69. Buckley, D. L.; Gustafson, J. L.; Van Molle, I.; Roth, A. G.; Tae, H. S.; Gareiss, P. C.; Jorgensen, W. L.; Ciulli, A.; Crews, C. M. *Angew. Chem., Int. Ed.* **2012**, *51*, 11463.
70. (a) Ji, H.; Stanton, B. Z.; Igarashi, J.; Li, H.; Martásek, P.; Roman, L. J.; Poulos, T. L.; Silverman, R. B. *J. Am. Chem. Soc.* **2008**, *130*, 3900; (b) Ji, H.; Li, H.; Martásek, P.; Roman, L. J.; Poulos, T. L.; Silverman, R. B. *J. Med. Chem.* **2009**, *52*, 779.
71. Yu, B.; Huang, Z.; Zhang, M.; Dillard, D. R.; Ji, H. *ACS Chem. Biol.* **2013**, *8*, 524.
72. Halgren, T. A. *J. Chem. Inf. Model.* **2009**, *49*, 377.
73. Zoete, V.; Meuwly, M.; Karplus, M. *Proteins* **2005**, *61*, 79.
74. Huang, Z.; Zhang, M.; Burton, S. D.; Katsakhyan, L. N.; Ji, H. *ACS Chem. Biol.* **2014**, *9*, 193.
75. (a) Reynès, C.; Host, H.; Camproux, A.-C.; Laconde, G.; Leroux, F.; Mazars, A.; Deprez, B.; Fahraeus, R.; Villoutreix, B. O.; Sperandio, O. *PLoS Comput. Biol.* **2010**, *6*, e1000695; (b) Hamon, V.; Brunel, J. M.; Combes, S.; Basse, M. J.; Roche, P.; Morelli, X. *MedChemCommun* **2013**, *4*, 797.
76. (a) Smith, M. C.; Gestwicki, J. E. *Expert Rev. Mol. Med.* **2012**, *14*, e16; (b) Cesa, L. C.; Patury, S.; Komiyama, T.; Ahmad, A.; Zuiderweg, E. R. P.; Gestwicki, J. E. *ACS Chem. Biol.* **1988**, *2013*, 8.
77. (a) Venkatesan, K.; Rual, J.-F.; Vazquez, A.; Stelzl, U.; Lemmens, I.; Hirozane-Kishikawa, T.; Hao, T.; Zenkner, M.; Xin, X.; Goh, K.-I.; Yildirim, M. A.; Simonis, N.; Heinzmann, K.; Gebreab, F.; Sahalie, J. M.; Cevik, S.; Simon, C.; de Smet, A.-S.; Dann, E.; Smolyar, A.; Vinayagam, A.; Yu, H.; Szeto, D.; Borick, H.; Dricot, A.; Klitgord, N.; Murray, R. R.; Lin, C.; Lalowski, M.; Timm, J.; Rau, K.; Boone, C.; Braun, P.; Cusick, M. E.; Roth, F. P.; Hill, D. E.; Tavernier, J.; Wanker, E. E.; Barabási, A.-L.; Vidal, M. *Nat. Methods* **2009**, *6*, 83; (b) Zhang, Q. C.; Petrey, D.; Deng, L.; Qiang, L.; Shi, Y.; Thu, C. A.; Bisikirska, B.; Lefebvre, C.; Accili, D.; Hunter, T.; Maniatis, T.; Califano, A.; Honig, B. *Nature* **2012**, *490*, 556.
78. Yildirim, M. A.; Goh, K.-I.; Cusick, M. E.; Barabási, A.-L.; Vidal, M. *Nat. Biotechnol.* **2007**, *25*, 1119.
79. (a) Levin, K. B.; Dym, O.; Albeck, S.; Magdassi, S.; Keeble, A. H.; Kleanthous, C.; Tawfik, D. S. *Nat. Struct. Mol. Biol.* **2009**, *16*, 1049; (b) Meenan, N. A. G.; Sharma, A.; Fleishman, S. J.; Macdonald, C. J.; Morel, B.; Boetzel, R.; Moore, G. R.; Baker, D.; Kleanthous, C. *Proc. Natl. Acad. Sci. U.S.A.* **2010**, *107*, 10080; (c) Kosloff, M.; Travis, A. M.; Bosch, D. E.; Siderovski, D. P.; Arshavsky, V. Y. *Nat. Struct. Mol. Biol.* **2011**, *18*, 846.